J Solid State Electrochem (2007) 11:847–852
DOI 10.1007/s10008-006-0231-y

ORIGINAL PAPER

# Effects of particle size on the electrochemical performances of a layered double hydroxide, $[Ni_4Al(OH)_{10}]NO_3$

**Meng Hu · Lixu Lei**

Received: 20 August 2006 / Revised: 21 September 2006 / Accepted: 4 October 2006 / Published online: 17 November 2006


**Abstract** In this paper, the electrochemical performances of a layered double hydroxide, $[Ni_4Al(OH)_{10}]NO_3$, of different particle sizes are studied. The results show that the particle size of the sample has evident effects on its discharge capacity at high current density, although a larger capacity may be observed for the bigger particles when they are discharged at lower current densities, e.g. 0.2 A $g^{-1}$. However, the capacity decreases more quickly than that of the sample in smaller particle size when the current density increases. For example, the discharge capacity of the smallest particle remains as high as 180 mAh·$g^{-1}$ even at very high current density, e.g. 4.0 A $g^{-1}$. The results also show that long time soaked electrodes in 7 mol $l^{-1}$ KOH have improved performance, especially for the hydrothermal samples. It also seems that there is an optimal size for materials, which can maintain their performance for longer time.

**Keywords** Layered double hydroxide (LDH) · $[Ni_4Al(OH)_{10}]NO_3$ · Particle size · Current density · Discharge capacity

## Introduction

New applications such as hybrid electric vehicles (HEVs), portable power tools and power backups require reliable secondary batteries of high energy and power density, which requires reliable electrode materials. Nickel hydroxides are widely used as cathode materials in primary and secondary alkaline batteries, therefore have received much attention [1, 2]. There are four kinds of nickel hydroxide found up to now, which are usually referred to as β-NiOOH, γ-NiOOH, β-$Ni(OH)_2$, α-$Ni(OH)_2$. Upon charge and discharge, β-NiOOH and β-$Ni(OH)_2$, γ-NiOOH and α-$Ni(OH)_2$ form electrochemical couples, respectively [3]. The former couple are currently used in commercial batteries, although the latter has two advantageous properties over the former. Firstly, unlike the β-NiOOH/β-$Ni(OH)_2$ couple, which turns out γ-NiOOH when it is overcharged and consequently leads to serious mechanical strain on cycling to the electrode, the γ-NiOOH/α-$Ni(OH)_2$ couple has much less mechanical strain because the α and γ phases have similar lattice constants. Secondly, the γ-NiOOH/α-$Ni(OH)_2$ couple has larger gravimetric capacity because its oxidation state is higher than the 3.5 of nickel in γ-NiOOH, which can be easily reached and stabilized [4, 5]. However, α-$Ni(OH)_2$ is thermodynamically unstable in strong alkaline medium and rapidly transforms to β-$Ni(OH)_2$ [3]. This characteristic prevents it from application in alkali batteries and therefore, many studies were carried out to stabilize α-$Ni(OH)_2$.

Researches showed that partial substitutions of Co, Fe, Al, Zn, Cr and Mn for Ni of nickel hydroxide could stabilize α-$Ni(OH)_2$ in the strong alkaline solution [6–13]. These substitutions have actually resulted in the formation of layered double hydroxides (LDHs). Those LDHs can be represented by a general formula, $\left[Ni_xM_y(OH)_{2(x+y)}\right]A^{n-}_{y/n}\cdot mH_2O$ [14] in which each M (usually trivalent cations) and Ni atom is octahedrally coordinated by 6 $OH^-$ anions and the octahedrons share six edges and form layers with anions A in the interlayer space. *x*, *y*, *m* and *n* are numbers determined by the stoichiometric composition of the compound.

M. Hu · L. Lei (✉)
School of Chemistry and Chemical Engineering,
Southeast University,
Nanjing 210096, People's Republic of China
e-mail: lixu.lei@seu.edu.cn

Among those LDHs, also called doped or stabilized $\alpha$-$Ni(OH)_2$ in literatures, Al doped compounds stand out because of their stability and electrochemical performances [14–21]. For example, $[Ni_{0.90}Al_{0.10}(OH)_2]$ $(NO_3)_{0.02}$ $(CO_3)_{0.04}$ had no degradation even if it had been soaked in 6 mol $l^{-1}$ KOH at room temperature for up to 2 months [22] and this was also found for $[Ni_{0.90}Al_{0.10}(OH)_2](NO_3)_{0.10}$ [17]. It was also found that the structure remains even after hundreds of charge–discharge cycles [16, 17]. Compared with the discharge capacity of β-$Ni(OH)_2$, which was found to be about 200 mAh $g^{-1}$ [10, 23], the capacities of Ni/Al LDHs containing 10%, 20% and 30% Al were found to be 320, 300 and 284 mAh $g^{-1}$,respectively, at a discharge rate of 0.3 C [17].

It was observed that better crystallinity of the $\left[Ni_xM_y(OH)_{2(x+y)}\right]^{y+}A^{n-}_{y/n}$ sample improves the capacity and half-discharge potential [24], which is contrary to the behaviors of the usual electrode material, β-$Ni(OH)_2$. This dependence on crystallinity can be explained by the reduction of polarization because of more ordered structure, which led to a faster solid state reaction [25]. The effect of particle size on the discharge performance of a nickel-metal hydride electrode was analyzed with a mathematical model, which clearly showed that the particle size affects the electrode performance significantly and that there is an optimal particle size for each discharge rate [26].

In spite of all these efforts, the effects of particle size on electrochemical performance are not well-known especially when the material is on heavy duty. As one of the researches carried out in our laboratory, this paper reports the electrochemical behaviors of $[Ni_4Al(OH)_{10}]NO_3$ of different sizes and crystallinities.

## Experiments

### Materials

All chemicals used in this research were purchased as analytical grade reagents and used without further treatments. Distilled water used in the experiments was boiled for 30 min to remove any dissolved gases.

### Preparation of $[Ni_4Al(OH)_{10}]NO_3$ of different sizes

$[Ni_4Al(OH)_{10}]NO_3$ was prepared by the co-precipitation method. Under vigorous stirring and Ar flow, a solution of 6.8 g $LiOH{\cdot}H_2O$ in distilled water was slowly dropped into a solution of 18.2 g $Ni(NO_3)_2{\cdot}6H_2O$ and 6.1 g $Al(NO_3)_3{\cdot}9H_2O$ in 150 ml distilled water at 100 °C in an hour. After the reaction mixture was stirred for another 10 h, it was filtered, washed and dried in vacuum at 50 °C. This is the sample 1.

Other samples were prepared as follows. A suspension of $[Ni_4Al(OH)_{10}]NO_3$ was prepared as above and directly transferred into a few Teflon-lined hydrothermal vessels and kept at certain temperature for 24 h. The solid product was then filtered, washed and dried in vacuum at 50 °C. The temperatures used were 125, 140, 150, 160, 170, 180, 190 and 200 °C and the samples prepared are denoted as 2 to 9, respectively.

### Physical characterizations

Elemental analysis of nickel and aluminium were performed by analytical service at Nanjing University by using a Jarrel-Ash J-A1100 ICP spectrometer. XRD patterns were recorded on a X'TRA diffractometer using Cu $K_\alpha$ ($\lambda$=1.5408 Å) radiation. Peaks of the XRD spectra were fitted with program Xfit (http://www.ccp14.ac.uk/tutorial/xfit-95/xfit.htm) to find the full width at half maximum (FWHM) and the diffraction angles ($2\theta$) of the first reflection. The Scherrer equation was then used to calculate the particle sizes.

### Electrochemical characterization

*Preparation of the electrodes* To obtain a paste, 28 mg of as prepared $[Ni_4Al(OH)_{10}]NO_3$, 80 mg of Ni powder, 20 mg of Co powder and a few drops of 5% aqueous polytetrafluoroethylene (PTFE) suspension were mixed thoroughly in an agate mortar. A piece of nickel foam sized 1.2×0.8 cm was sandwiched with the paste using a spatula, dried at 80 °C for 24 h, then pressed at 20 MPa for 1 min to assure good electrical contact between the substrate and the active material. The electrode had been immersed in 7 mol $l^{-1}$ KOH for 24 h before use.

*Electrochemical characterizations* Using a CHI660b electrochemical interface controlled by a computer, electrochemical characterizations were performed in a three-compartment electrolysis cell at room temperature under tiny Ar flow. A piece of nickel foam was employed as the counter electrode, HgO/Hg electrode in 7 mol $l^{-1}$ KOH as the reference electrode and 7 mol $l^{-1}$ KOH as the electrolyte.

Cyclic voltammetric measurements were carried out by cycling the electrodes at a scan rate of 10 mV $s^{-1}$ from 0.1 to 0.8 V vs the HgO/Hg electrode. The charge–discharge cycles were carried out at selected constant currents.

## Results

### Chemical composition of the samples

Three selected samples, including the sample co-precipitated at 100 °C (sample 1), and two samples hydrothermally

treated at 180 °C (sample 7) and 200 °C (sample 9) were analyzed by ICP; the results are shown in Table 1. Molar ratios of nickel to aluminum are all around 3.9, which are consistent with the initial ratio of the starting materials. However, the contents of the co-crystallized water molecules decrease as the reaction temperature rises.

## XRD characterizations

Figure 1 shows the XRD patterns of $[Ni_4Al(OH)_{10}]NO_3$, which are in agreement with literatures [9, 14, 24]. Table 2 shows the particle sizes of the samples obtained according to the Scherrer equation. Figure 2 shows the relationship of particle size to temperature used in hydrothermal treatments, which reveals that particle size increases as hydrothermal temperature increases. The *d* spacings of the samples are all around 0.795 nm. Therefore, hydrothermal treatments at higher temperatures make the samples more crystallized without changing the Ni/Al ratio.

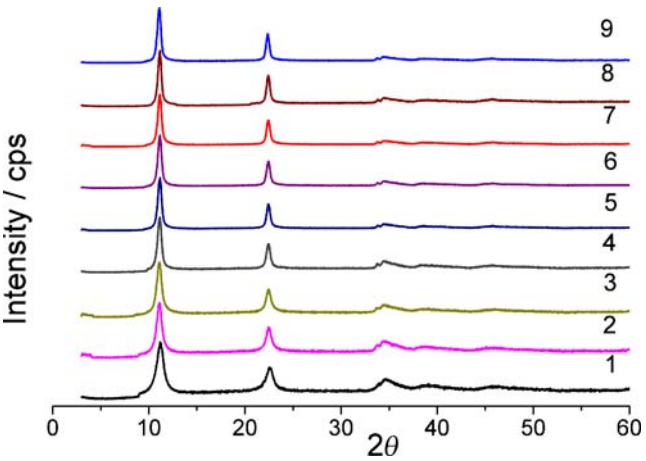


**Fig. 1** XRD patterns of the nine samples of $[Ni_4Al(OH)_{10}]NO_3$. *1* is the co-precipitated sample; *2* to *9* are the samples hydrothermally treated at 125, 140, 150, 160, 170, 180, 190 and 200 °C, respectively

## Electrochemical characterizations

### *Cyclic voltammetry*

Figure 3 shows the cyclic voltammetric curves of samples 1, 7 and 9 after 20 cycles of charges and discharges, together with a parallel experiment in which the electrode contains electrochemically inert $[Mg_2Al(OH)_6]NO_3$ instead of $[Ni_4Al(OH)_{10}]NO_3$, at a scan rate of 0.20 mV $s^{-1}$. It can be seen that voltammetric curves of the three samples are basically the same, but the sample prepared at 200 °C exhibits some abnormality. The reason is unclear, but it is possible that there is some unknown structural changes since the sample suffered the highest hydrothermal temperature. Furthermore, the effect of the conductive agents, nickel and cobalt powder, on the electrochemical performances are small and may be neglected.

### *Charge–discharge cyclic performances at high current densities*

Figure 4 shows the variations of the discharge capacity of the selected samples as a function of the cycle number. It seems that co-precipitated sample 1, which has the smallest particle size, has highest initial discharge capacity, but it soon reaches its maximum. However the hydrothermal samples, which have bigger particle sizes and more regular structures, have better and better discharge capacities as the cycle number increases. More importantly, the bigger the particle size is, the bigger the increase in capacity is.

To examine the stability of the samples to strong alkali solution, the above electrodes had been soaked in the electrolyte (7 mol $l^{-1}$ KOH) for 30 days. The electrodes' performance in the charge–discharge cycles and discharge capacity at different discharge current densities were re-examined.

Figure 5 shows the variations of discharge capacity as a function of the cycle number for another 100 cycles after the electrodes had been soaked in 7 mol $l^{-1}$ KOH for 30 days. It can be seen that (1) all the samples has better discharge capacities than before. For example, the discharge capacity of co-precipitated sample 1 increased from 240 mAh $g^{-1}$ of the last cycle before the soak to 278 mAh $g^{-1}$ of the first cycle after the soak; while the hydrothermal samples 7 and 9 increased from 230 and 258 mAh $g^{-1}$, respectively, to 270 mAh $g^{-1}$. Furthermore, the interruption of the cycling process could also improved the capacity, though the interruptions have different effects to different samples; (2) the co-precipitated sample 1 continues its evident decay process as it had started in the former

**Table 1** Chemical composition of the prepared $[Ni_4Al(OH)_{10}]NO_3$

| Samples | Al (wt.%) | | Ni (wt.%) | | Mole ratio of Ni to Al | Stoichiometric formula |
|---|---|---|---|---|---|---|
| | Found | Calculated | Found | Calculated | | |
| 1 | 4.87 | 4.85 | 41.2 | 41.1 | 3.89 | $Ni_{3.9}Al(OH)_{9.8}NO_3{\cdot}4.0H_2O$ |
| 7 | 5.08 | 5.10 | 43.1 | 43.2 | 3.90 | $Ni_{3.9}Al(OH)_{9.8}NO_3{\cdot}2.5H_2O$ |
| 9 | 5.15 | 5.18 | 44.0 | 44.0 | 3.93 | $Ni_{3.9}Al(OH)_{9.8}NO_3{\cdot}2.0H_2O$ |

**Table 2** XRD data and calculated particle sizes

| Samples | FWHM (°) | 2θ (°) | *d* value | Particle size (nm)* |
|---|---|---|---|---|
| 1 | 0.8987 | 11.18 | 7.91 | 11.4 |
| 2 | 0.6598 | 11.09 | 7.97 | 16.1 |
| 3 | 0.6115 | 11.09 | 7.97 | 17.4 |
| 4 | 0.5006 | 11.12 | 7.95 | 20.9 |
| 5 | 0.4645 | 11.13 | 7.94 | 22.5 |
| 6 | 0.4702 | 11.12 | 7.95 | 22.3 |
| 7 | 0.4562 | 11.14 | 7.94 | 22.8 |
| 8 | 0.4040 | 11.13 | 7.94 | 25.8 |
| 9 | 0.4466 | 11.07 | 7.99 | 24.0 |

*Particle sizes were calculated by using the Scherrer equation, $D=K\lambda/\beta\cos\theta$ where $K=0.89$, $D$ is the particle size, $\lambda=0.15406$ nm, $\beta$ is the FWHM in radians and $\theta$ is the Bragg angle of the reflection.

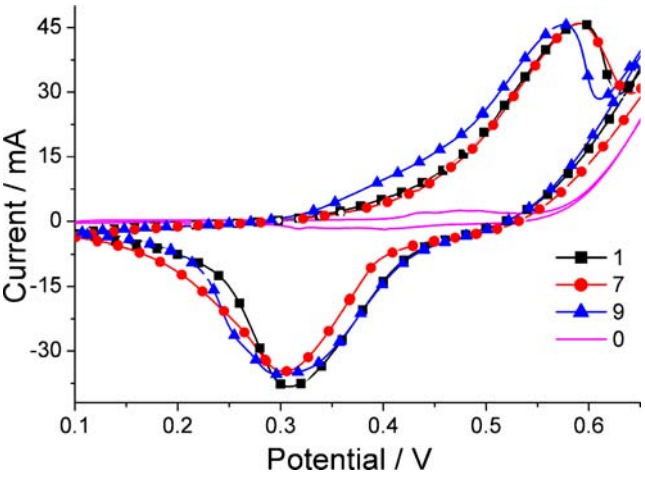


**Fig. 3** Cyclic voltammetric curves of $[Ni_4Al(OH)_{10}]NO_3$ as prepared by co-precipitation at 100 °C, sample 1, 11 nm; hydrothermal treatment at 180 °C, sample 7, 23 nm hydrothermal treatment at 200 °C, sample 9, 24 nm and conductive materials, sample 0

20 cycles; however, the hydrothermal samples kept their discharge capacities much better even when the cycle number increases up to 100. Sample 7 kept its discharge capacity even better than sample 9. Since sample 7 is only a little bit smaller than sample 9, which may be insignificant, we guess that hydrothermal temperature may have some impact on the performance. Further investigation is being done to verify the possible reason for that phenomenon.

We believe that the above two results show that the permeation of electrolyte into the electrode has an important effect on the discharge capacity, since there could not exist other factors during the soaking process. Therefore, adjusting the components of the electrode to make better contact between the active material and the electrolyte should be paid more attention to.

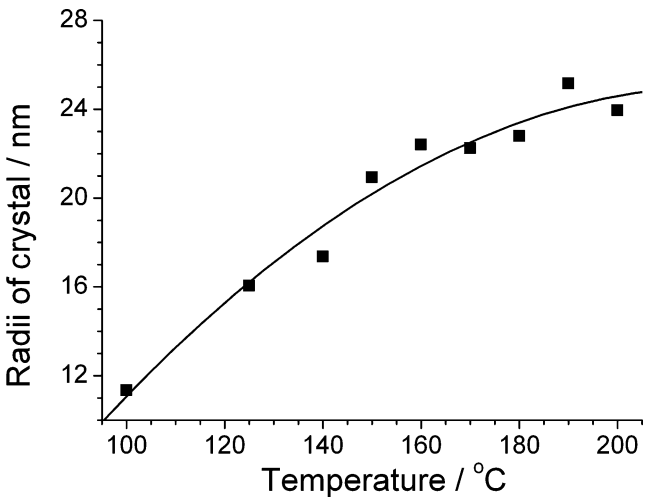


**Fig. 2** The relationship of particle size with reaction temperature (the smooth curve is a polynomial fit just for guidance)

*The performance under high power outputs*

High performance batteries for heavy duty applications such as in electric vehicles require high power output and input. It is especially important that the electrode should discharge more energy under the circumstance. Therefore, we have investigated the discharge capacities of the selected $[Ni_4Al(OH)_{10}]NO_3$ electrodes at high current density discharges. The electrodes were all overcharged at a constant current density of 1,428 mA $g^{-1}$ then discharged at different current densities. This design can fully charge the electrode in less than 15 min and fully discharged in a few minutes up to a couple of hours. Figure 6 shows the curves of the discharge capacities of the samples vs the discharge current densities, including both the electrodes

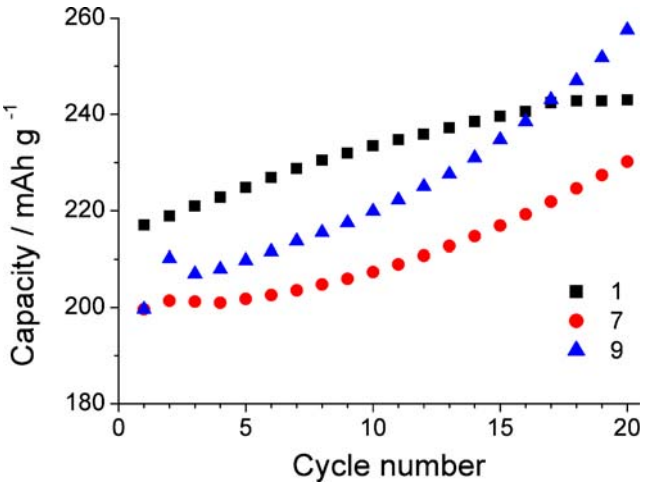


**Fig. 4** Variations of discharge capacity as a function of the cycle number in the initial 20 cycles of the selected samples. Each cycle includes a charge at 40 mA (1.40 A $g^{-1}$) and a discharge at 20 mA (0.71 A $g^{-1}$)

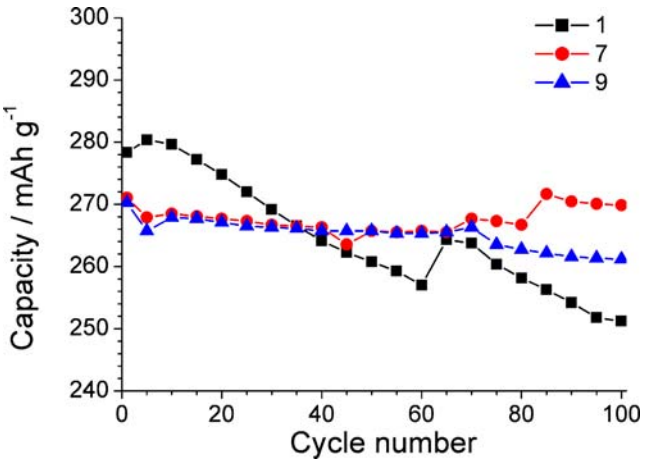


**Fig. 5** Variations of the discharge capacity of the selected samples as a function of the cycle number for another 100 cycles after the electrodes had been soaked in 7 mol $l^{-1}$ KOH for 30 days. Each cycle includes a charge at 40 mA (1.4 A $g^{-1}$) and a discharge at 20 mA (0.71 A $g^{-1}$). The sudden rises, e.g. cycle 64 for sample 1 and cycles 70 and 84 for sample 7 were caused by the interruption of the cycling process for about 10–12 h

that experienced the initial 20 cycles and the ones that experienced the latter 100 cycles.

It can be seen from Fig. 6 that the discharge capacity of each sample decreases as the discharge current density increases as usual, but the history of a sample has a strong impact on the performance at high power output. For example, after the former 20 cycles, the co-precipitated sample 1 has the best performance while the 200 °C hydrothermally treated sample 9 has the worst performance. It seems that higher hydrothermal temperature, which also means bigger particle size, leads to worse performance at high power output after the former charge–discharge cycles. However, after the electrodes had been soaked in KOH for 30 days and then cycled another 100 times, the medium sized sample 7 turns out to be the best and sample 1 the worst!

Figure 7 shows the increments of the discharge capacities of the electrodes before and after the latter soaking and 100 cycles as a function of the discharge current density. It can be seen that the long time soaking and high cycle number make the discharge capacity increase for the hydrothermally treated samples, but not for the co-precipitated sample.

## Discussion

From the above results, we can summarize that the particle size, crystallinity and history of the sample have profound influence on the performance of the electrode at high power output. (1) The crystallinity of the sample affects the cyclic life of the electrode: better crystallized sample decays slower and lasts longer; (2) smaller crystalline samples may, but not always, have better performance upon high power output; (3) well-wetted electrode, which means better contact between the active material and the electrolyte, has better performance.

It is believed that particle size has an important effect on high power output applications because any electrode process must include rapid transfers of both electrons and ions. When the electrode is discharged or charged at low current, it does not require rapid motion of both electrons and ions. However, when the electrode is discharged or charged at high current, any delay or resistance of electron and ion movements will certainly raise the polarization of electrode, which impairs the performance of the electrode. For a layered double hydroxide electrode, when it is

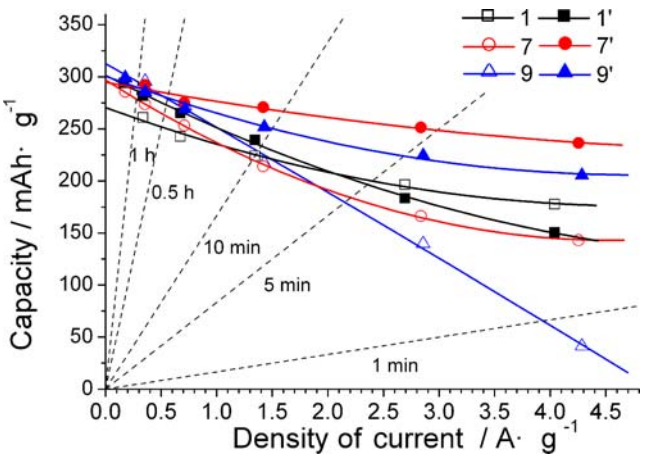


**Fig. 6** Variations of the discharge capacity of the selected samples as a function of their discharge current density. The *1*, *7*, *9* are the electrodes after the former 20 cycles and the *1′*, *7′*, *9′* are the electrodes after the latter 100 cycles. *Solid lines* are polynomial fits, for guidance and *dash lines* are the ratio of the capacity to the current density

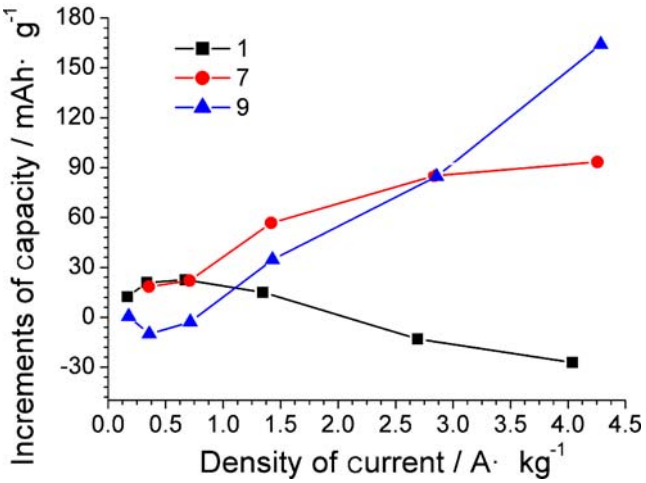


**Fig. 7** Variant increments of the discharge capacity of each sample after 100 cycles from the capacity after 20 cycles as a function of their discharge current density

charged or discharged, some anions must intercalate into or de-intercalate out of the interlayer spaces. Therefore, the intercalation/de-intercalation speed of the anions has a strong impact on the performance of the electrode. Since it is more difficult to diffuse anions in between the layers than the anions outside of the layers, the bigger the diffusion distance in the interlayer space, the slower the anions migrate out of the interlayer space. Consequently, bigger particle size is negative to the high power output. This is also found in a mathematical analysis of the metal hydride electrode [26].

On the other hand, a regular structure is positive to the rapid movements of interlayer anions because it makes the anions encounter less random scattering. The less random scattering has two effects on the present system: one is the less resistance to anion movements and the other is that it makes the structure lasts longer. It should be remembered that fast movement of anions colliding with the structure can make the structure fragile and broken and smaller particles are incapable of suffering such frequent and strong collisions. Therefore, the small size and well-crystallized sample 7 behaves better than the smaller size but badly crystallized sample 1 and the well-crystallized but bigger size sample 7.

Still, there must be a rapid exchange of anions between the solid electrode material and the electrolyte to make the electrode process fast-going. The soaking of the electrodes in alkali solution for 30 days certainly makes such an exchange easier, thus improving the performance.

## Conclusions

In conclusion, to make high performance electrode for heavy duty applications, well-crystallized active materials of smaller size should be prepared since it allows both the rapid movements and less distance of diffusion in between the layers of the interlayer anion. Good contact of the active material with the current collector and electrolyte is also very important.

**Acknowledgements** We would like to thank the Jiangsu Province Fundamental Research Project (Natural Science Fund) BK2004071 and the Scientific Research Foundation for the Returned Overseas Chinese Scholars, State Education Ministry for the financial support.

## References

1. Linden D (1995) Handbook of batteries. McGraw-Hill, New York
2. Srinivasan V, Weidner JW, White RE (2000) J Solid State Electrochem 4:367
3. Bode H, Dehmelt K, Witte J (1966) Electrochim Acta 11:1079
4. Barnard R, Randell CF, Tye FL (1980) J Appl Electrochem 10:109
5. Corrigan DA, Knight SL (1989) J Electrochem Soc 136:613
6. Faure C, Delmas C, Willmann P (1991) J Power Sources 36:497
7. Demourgues-Guerlou L, Delmas C (1993) J Power Sources 45:281
8. Indira L, Dixit M, Kamath PV (1994) J Power Sources 52:93
9. Kamath PV, Dixit M, Indira L, Shukla AK, Kumar VG, Munichandraiah N (1994) J Electrochem Soc 141:2956
10. Dixit M, Jayashree RS, Kamath PV, Shukla AK, Kumar VG, Munichandraiah N (1999) Electrochem Solid State Lett 2:170
11. Jayashree RS, Vishnu Kamath P (2002) J Power Sources 107:120
12. Chen H, Wang JM, Zhao YL, Zhang JQ, Cao CN (2005) J Solid State Electrochem 9:421
13. Wu MY, Wang JM, Zhang JQ, Cao CN (2005) J Solid State Electrochem 10:411
14. Ehlsissen KT, Delahaye-Vidal A, Genin P, Figlarz M, Willmann P (1993) J Mater Chem 3:883
15. Liu B, Wang XY, Yuan HT, Zhang YS, Song DY, Zhou ZX (1999) J Appl Electrochem 29:855
16. Wang CY, Zhong S, Konstantinov K, Walter G, Liu HK (2002) Solid State Ion 148:503
17. Hu WK, Noreus D (2003) Chem Mater 15:974
18. Pan T, Wang JM, Zhao YL, Chen H, Xiao HM, Zhang JQ (2003) Mater Chem Phys 78:711
19. Zhang HB, Liu HS, Cao XJ, Li SJ, Sun CC (2003) Mater Chem Phys 79:37
20. Roto R, Yamagishi A, Villemure G (2004) J Electroanal Chem 572:101
21. Zhao Y, Liang J (2005) J Adv Mater 37:49
22. Caravaggio GA, Detellier C, Wronski Z (2001) J Mater Chem 11:912
23. Dixit M, Kamath PV, Kumar VG, Munichandraiah N, Shukla AK (1996) J Power Sources 63:167
24. Sugimoto A, Ishida S, Hanawa K (1999) J Electrochem Soc 146:1251
25. Jayashree RS, Kamath PV, Subbanna GN (2000) J Electrochem Soc 147:2029
26. Heikonen JM, Ploehn HJ, White RE (1998) J Electrochem Soc 145:1840